



Effects of rainfall rate on physical characteristics of outdoor noise from the viewpoint of outdoor acoustic mass notification system

Sato, Hayato
Kurusu, Kiyohiro
Morimoto, Masayuki
Maeda, Mitsuki

(Citation)

Applied Acoustics, 172:107616

(Issue Date)

2021-01-15

(Resource Type)

journal article

(Version)

Accepted Manuscript

(Rights)

© 2020 Elsevier Ltd. All rights reserved.

This manuscript version is made available under the CC-BY-NC-ND 4.0 license

<http://creativecommons.org/licenses/by-nc-nd/4.0/>

(URL)

<https://hdl.handle.net/20.500.14094/90009294>



Effects of rainfall rate on physical characteristics of outdoor noise from the viewpoint of outdoor acoustic mass notification system

Hayato Sato^{a,*}, Kiyohiro Kurisu^b, Masayuki Morimoto^a, Mitsuki Maeda^a

^a*Environmental Acoustics Laboratory, Department of Architecture, Graduate School of Engineering, Kobe University, Rokko, Nada, Kobe 657-8501, Japan*

^b*TOA Corporation, Minatojima-Nakamachi, Chuo-ku, Kobe 650-0046, Japan*

Abstract

In Japan, there are many natural disasters that often expose residents to the risk of serious damage. To minimize such damage, the Japanese government has built a disaster information network using a radio system, and as part of it, an outdoor acoustic mass notification system is routinely operated. However, its intelligibility may be reduced by outdoor noise, which is increased by rainfall. In the present study, long-term surveys of rainfall rate and outdoor noise were conducted at four sites with different surrounding environments and the relationship between them was analyzed to clarify the effects of the rainfall rate on the physical characteristics of outdoor noise. The results indicated that the median sound pressure level for each 1/3 octave band increased with increasing rainfall rate, mainly above mid-frequencies of around 500 Hz to 1 kHz, though the frequency at which the level began to rise depended on the time period and site. Furthermore, a newly proposed macroscopic model for estimating the sound pressure level of outdoor

*Corresponding author. Tel./fax: +81 78 803 6052.

Email address: hayato@kobe-u.ac.jp (Hayato Sato)

noise under rainy conditions indicated that the distance from the loudspeaker of the system to ensure a certain speech-to-noise ratio could be significantly reduced by heavy rainfall.

Keywords: Outdoor noise, Mass notification system, Raindrop collision, Speech intelligibility

1. Introduction

In Japan, there are many natural disasters such as earthquakes, typhoons, heavy rain, and tsunamis, which expose residents to the risk of serious damage. To minimize such damage, it is necessary to quickly and accurately transmit disaster information to residents. The Japanese government has built a disaster information network at the national, prefectural, and local levels that uses a radio system, and as part of it, sound information is routinely transmitted over a wide area using an outdoor acoustic mass notification system. In general, a system is adopted in which a slave station consisting of a radio receiver and loudspeakers is installed on a building roof or a dedicated pole and the sound information transmitted from a master station is radiated from the loudspeakers with a high sound pressure level (SPL).

It is well known that outdoor sound propagation is affected by weather conditions. For example, the effects of the vertical distribution of wind speed and temperature on long-distance sound propagation have been studied in detail. When considering sound information transmission, it is necessary to estimate the signal-to-noise ratio, which determines intelligibility. This means that not only the SPL of the sound carrying information transmitted from far away to a listening point but also the SPL of background noise at the point should be estimated. In

20 other words, the effects of weather on background noise should be investigated.

21 In recent years, in Japan, damage caused by sudden and localized heavy rain
22 that is difficult to predict has increased. In such cases, it is necessary to transmit
23 evacuation information. The transmission of evacuation information using an
24 outdoor acoustic mass notification system can be effective because an immediate
25 response to such an unexpected situation is possible. However, during rainfall, the
26 SPL and frequency characteristics of outdoor noise change owing to the sound of
27 raindrops colliding with surfaces, and the intelligibility of evacuation information
28 will decrease.

29 There have been several studies on noise generated by the collision of
30 raindrops, for example, vegetation noise[1] and roof noise[2–6]. Furthermore,
31 changes in traffic noise when a road surface is wet have also been studied[7–10].
32 Outdoor noise during rainfall is a combination of these factors, and therefore
33 the effects of rainfall will depend on the environment around the measurement
34 point. However, no study could be found on how rainfall changes the physical
35 characteristics of such complex outdoor noise.

36 The purpose of the present study is to clarify the effects of the rainfall rate,
37 which is the main parameter of rainfall, on the physical characteristics of outdoor
38 noise. As a case study, a long-term survey of rainfall and outdoor noise was
39 conducted at four sites with different surrounding environments. On the basis of
40 the results, the change in outdoor noise due to rainfall and how the change affects
41 the speech intelligibility of information transmitted by an outdoor acoustic mass
42 notification system were analyzed.

43 2. Methods

44 Measurements were performed at four sites in Hyogo Prefecture, Japan. The
45 measurement sites were selected to satisfy the following conditions:

- 46 (1) Permission to use a building or a lot including a stable electrical power
47 supply was obtained from the owner.
- 48 (2) Measurement equipment could be physically isolated from pedestrians.
- 49 (3) The characteristics of surfaces on which raindrops impact were different at
50 each site.

51 Table 1 shows a summary of the measurement sites. Figure 1 shows satellite
52 photos of the measurement sites obtained from Google Earth. The red circles in
53 the photos indicate the measurement points.

54 [Table 1 about here.]

55 [Figure 1 about here.]

56 The measurement equipment consisted of a weather measuring device and a
57 noise measuring device. Both were connected to a tablet PC (Microsoft, Surface
58 3), and measurement data were uploaded continuously to cloud storage (Dropbox)
59 via the PC. The weather measuring device (Davis, VantagePro2) recorded the
60 temperature, relative humidity, wind speed, and rainfall rate every minute. The
61 noise measurement was performed using a sound level meter (Rion, NL-21) with
62 an all-weather windscreen (Rion, WS-03). The AC output of the sound level meter
63 was transmitted to the PC using an audio unit (Roland, UA-11Mk2). L_{Aeq} and L_{eq}
64 in each 1/3 octave band were calculated from the AC output every minute using

65 the first 30 s of the sample. Time stamps were also added to both weather and
66 noise data. Therefore, a synchronized set of weather and noise data was obtained
67 every minute. Figure 2 shows the equipment installed at site 2 as an example.

68 [Figure 2 about here.]

69 The equipment was operated continuously from early October to the end of
70 November in 2015, though the measurement period varied somewhat among the
71 sites. Note that missing observations occurred intermittently at every site because
72 of the unexpected shutdowns of the PC or the forced terminations of the software
73 used to calculate sound levels. Table 2 shows the measurement periods and the
74 numbers of samples of weather and noise data successfully recorded.

75 [Table 2 about here.]

76 **3. Results and discussion**

77 *3.1. Rainfall rate*

78 Figure 3 shows temporal sequences of the rainfall rate every minute for
79 each site. The unit of rainfall rate is mm/h, and the rainfall rate was estimated
80 from one-minute measurements. Periods colored in grey represent missing
81 observations. Roughly, rainfall was simultaneously observed at all of the sites,
82 because the distance among the sites was 16 km at most. Note that rainfall rates
83 of more than 40 mm/h, which is a typical threshold for a heavy rainfall warning in
84 Japan and is classified as *Heavy* in ISO 10140-5:2010[11], were observed several
85 times in the measurement periods, though such heavy rainfall lasted for a short
86 time.

[Figure 3 about here.]

Table 2 also shows the numbers of samples with rainfall and with a rainfall rate of more than 40 mm/h for each site. In the following sections, the samples are classified into two groups: *without rainfall* for the samples with zero rainfall rate, and *with rainfall* for the samples with nonzero rainfall rate.

3.2. Outdoor noise without rainfall

The physical characteristics of outdoor noise for *without rainfall* are required as a reference to analyze the effects of rainfall on outdoor noise. In this section, factors of outdoor noise for *without rainfall* at the sites are investigated to classify the measured samples. The main noise sources at the sites were traffic noise, aircraft noise, and sound from pedestrians. In many cases, the frequency characteristics of these sources are broadband spectra rather than line spectra. Therefore, L_{Aeq} for each sample was first analyzed as a representative measure.

3.2.1. Effect of measurement time

Figure 4 shows the time sequence of L_{Aeq} from 2nd (Mon.) to 8th (Sun.) November 2015 for each site as an example. Discontinuous periods were missing observations or *with rainfall*. Daily cycles of L_{Aeq} were clearly found and the time pattern for each cycle was similar for all days of the week at each site.

[Figure 4 about here.]

However, the dynamic ranges of L_{Aeq} variation in each daily cycle were different at different sites. The dynamic ranges for sites 1 and 2 were around 20 dB (site 1: 40–60 dB, site 2: 50–70 dB), excluding some sporadic high L_{Aeq} values. The range for site 4 was around 35 dB (40–75 dB), which was the widest

among the sites. Sites 2 and 4 had similar features, as shown in Table 1, and the main noise source at these sites was road traffic noise. The decrease in the lower limit of the range of site 4 relative to site 2 might have been related to the fact that the traffic of the road beside site 2 is heavier than that beside site 4. The microphone of site 4 was installed at a lower position than that of site 2, and the distance between the microphone and the road can explain the increase in the upper limit of site 4 relative to site 2.

The daily cyclic pattern for site 3 was different from those for the other sites at first glance. Samples with L_{Aeq} of 60 to 65 dB were frequently observed from 07:00 to 21:00. An airport is located near sites 2, 3, and 4, and the normal take-off flight path of the airport was close to site 3. Because of the location of site 3 and the flight schedule of the airport, it is likely that the L_{Aeq} for this site values were strongly affected by aircraft noise.

Therefore, the samples with a strong effect of aircraft noise were extracted with reference to the L_{eq} of the low-frequency band, which is hardly affected by rainfall, and they were excluded from the analysis. In particular, the samples with L_{eq} of more than 60 dB in the 63 Hz band were excluded for site 3 only.

Figure 5 shows the median and 90% range of L_{Aeq} for the *without rainfall*. The statistics were calculated hourly for each site. The median of L_{Aeq} started to rise after 04:00, and remained high between 07:00 and 17:00, and then decreased gradually. This tendency was common to all of the sites. Although the width of the 90% range had different dynamic ranges at different sites, its time sequence showed the same trend as the median of L_{Aeq} . The differences between the maximum and minimum values of the median of L_{Aeq} were 8.4, 11.2, 7.4, and 20.9 dB for sites 1 to 4, respectively.

[Figure 5 about here.]

It can be assumed that the effect of rainfall on outdoor noise depends on the ratio of the energy of outdoor noise under no rainfall conditions to that of sounds caused by rainfall. Therefore, the wide dynamic ranges of the median of L_{Aeq} indicate that the outdoor noise obtained here should be classified by the time of day of the measurement. Hereafter, data are analyzed in two periods of time, 01:00–04:59 (*NT*) and 07:00–17:59 (*DT*), because the statistics of L_{Aeq} in these periods were temporally flat relative to those in other periods of time as shown in Fig. 5.

3.2.2. Effects of other weather parameters

As described in section 2, temperature, relative humidity, and wind speed were measured as weather parameters other than rainfall rate. The relationships between L_{Aeq} and the parameters for *without rainfall* samples were analyzed. It was found that L_{Aeq} was not systematically affected by temperature and relative humidity; however, L_{Aeq} increased with increasing wind speed. The main sources of the wind noise are thought to be the rustling of leaves[1] (sites 1 and 2) and air turbulence[12, 13] (all sites).

The weather measuring device used in the present study records wind speed in steps of 1 mi/h. In the present study, the unit of the wind speed was converted from mi/h to m/s as follows: (1) multiplied by 1609 to convert miles to meters, (2) divided by 3600 to convert hours to seconds, and (3) rounded to the first decimal place. Figure 6 shows the median of L_{Aeq} as a function of wind speed, and the cumulative frequency of wind speed for each site and time period. The wind noise measured by Lin *et al.*[13] with the same wind screen (Rion, WS-03) is

also shown in Fig. 6. Lin *et al.* demonstrated that the wind speed in the wind screen was 0.0 m/s and that the maximum increase in L_{Aeq} was 0.7 dB unless the outside wind speed exceeded 2.0 m/s. In the data measured in the present study, the maximum median of L_{Aeq} relative to that at zero wind speed was also around 1 dB regardless of the site and time period unless the wind speed exceeded 2.0 m/s. The median of L_{Aeq} began to increase in some cases when the wind speed exceeded 2.0 m/s. However, the cumulative frequency of the wind speed showed that the samples with a wind speed less than 2.0 m/s accounted for more than 90% of the samples in many cases. Although the samples with a wind speed more than 2.0 m/s were more frequently found at sites 2 and 3 in *DT* than in other cases, the slopes of L_{Aeq} with respect to the wind speed in the two cases were shallow.

From the above, it is considered that the effects of temperature, relative humidity, and wind speed were negligible as a whole, and the classification of samples based on these parameters was not carried out in the following analyses.

[Figure 6 about here.]

3.2.3. Frequency characteristics of L_{eq} without rainfall

The frequency characteristic of *without rainfall* for the two time periods (*NT* and *DT*) was obtained as a reference for analyzing the effect of rainfall. Figure 7 shows the median and 90% range of L_{eq} for each 1/3 octave band.

[Figure 7 about here.]

At all sites, the statistics of L_{eq} for *DT* was higher than that for *NT*, but there was no significant difference in frequency characteristic between *NT* and *DT*.

The frequency characteristics can be roughly divided into two types. For sites 1 and 3, over a wide frequency range, the median of L_{eq} decreased about 3 to

183 4 dB with a doubling of the center frequency of 1/3 octave band. This slope was
184 similar to that for the type of noise referred to as 'red noise' which has amplitude
185 inversely proportional to the frequency. For sites 2 and 4, the median of L_{eq} was
186 almost flat at 1.25 kHz or less and decreased with increasing frequency in the
187 higher range. As shown in Table 1, sites 2 and 4 were beside a main road, and
188 their frequency characteristics agreed with that of road traffic noise[14]. From the
189 above, it can be considered that the frequency characteristics of sites 2 and 4 were
190 almost completely determined by road traffic noise from the nearby major road.
191 For sites 2 and 4, the absolute values of the median of L_{eq} were almost identical
192 between the sites for *DT*, but the absolute values of the median of L_{eq} for site 4
193 were lower than those of site 2 for *NT*. It is reasonable to conclude that this was
194 due to the difference in road traffic in *NT*. Because at the upper limit of the 90%
195 range, this can be regarded as the result when the traffic was heavy, there was no
196 significant difference between the two sites for *NT*.

197 The median and the lower limit of the 90% range for site 1 in *DT* might have
198 an intermediate characteristic between the road traffic noise type and the red noise
199 type. It is considered that they were affected by distant traffic noise when the
200 surroundings were quiet, as the altitude of site 1 was about 120 m and the distant
201 city could be seen.

202 3.3. Outdoor noise with rainfall

203 The sound power of rain noise from a roof surface increases with increasing
204 rainfall rate as the number of collisions per unit time increases. For artificial rain,
205 the noise level increases by about 10 dB per 10-fold increase in rainfall rate[5].
206 For natural rain, the noise level increases by 10 dB or more per 10-fold increase
207 in rainfall rate because the radius and terminal velocity of raindrops increase

208 with the rainfall rate. Specifically, the increase is about 15 to 20 dB[2, 3].

209 The sounds caused by rainfall are not only the rain noise on roofs. However,
210 the relationship between their total SPL and the rainfall rate is expected to be a
211 logarithmic function similarly to the case of rain noise on roofs. Considering not
212 only the logarithmic relationship but also the balance of the number of samples
213 included in each classification, the rainfall rate was divided into the five classes
214 shown in Table 3. The numbers of *with rainfall* for each classification, site, and
215 time period are also shown in Table 3. For site 3, the samples with L_{eq} of more
216 than 60 dB at 63 Hz band were excluded as in the case of *without rainfall*.

217 [Table 3 about here.]

218 Table 4 shows the medians of rainfall rate, temperature, and relative humidity,
219 and the average wind speed for each classification of rainfall rate. For the
220 wind speed, the average was used as a representative value because of the lower
221 measurement resolution. The average wind speed was less than 2.0 m/s under
222 almost all conditions; thus, the effect of the wind speed on the results was
223 negligible.

224 [Table 4 about here.]

225 3.3.1. Relationship between rainfall rate and L_{Aeq}

226 For each classification in Table 3, statistics of the rainfall rate and L_{Aeq} were
227 calculated. Figure 8 shows the relationship between them in scattergrams. The
228 rainfall rate on the horizontal axis has a logarithmic scale. For reference, the
229 statistics of L_{Aeq} for *without rainfall* are also shown in Fig. 8.

230 [Figure 8 about here.]

231 For many combinations of time period and site, the statistics of L_{Aeq} tended
 232 to increase linearly with the logarithmic rainfall rate. There were differences in
 233 slope among the combinations. The slope became steeper as L_{Aeq} for *without*
 234 *rainfall* decreased. For example, at site 1, the median of L_{Aeq} was 44.3 dB and the
 235 difference between the maximum and the minimum rainfall rates was 10.5 dB for
 236 *NT*, while the median of L_{Aeq} was 51.5 dB and the difference was 5.1 dB for *DT*.

237 In order to analyze the SPL of the sounds caused by rainfall, $L_{\text{CRF}}(RR)$ defined
 238 by Eq. 1 was obtained as

$$L_{\text{CRF}}(RR) = 10 \log_{10} \left(10^{L_{\text{Aeq}}(RR)/10} - 10^{L_{\text{Aeq}}(0)/10} \right), \quad (1)$$

239 where $L_{\text{Aeq}}(0)$ is the median of L_{Aeq} without rainfall and $L_{\text{Aeq}}(RR)$ is the median
 240 of L_{Aeq} when the median of the rainfall rate is RR . Figure 9 shows scattergrams
 241 of $L_{\text{CRF}}(RR)$ and the median of the rainfall rate for each classification shown in
 242 Table 3. Trends were divided into two groups, sites 1 and 3 and sites 2 and 4,
 243 from the viewpoint of differences due to the time period.

244 [Figure 9 about here.]

245 *Sites 1 and 3*

246 In the group of sites 1 and 3, the absolute value of $L_{\text{CRF}}(RR)$ was not strongly
 247 affected by the time period. However, the slope of $L_{\text{CRF}}(RR)$ plotted against
 248 rainfall rate was steeper for *NT* than for *DT*. The slopes were similar to that for the
 249 rain noise on roofs, which is 10 dB or more per 10-fold increase in rainfall rate,
 250 except for *DT* at site 1. This indicates that the sounds caused by rainfall at the
 251 sites primarily consisted of those caused by the collision of raindrops with other
 252 objects.

253 For both time periods, the slopes were steeper for site 3 than for site 1. One
254 reason why the slopes differed between sites 1 and 3 might have been the effect of
255 traffic noise in site 1 as mentioned in 3.2.3. As an alternative reason, it is possible
256 to consider the difference in the type of object with which raindrops collide. The
257 main object was leaves of surrounding trees for site 1, whereas it was gravel on
258 the ground for site 3. These objects differed in shape and mass, and it is clear
259 from the theory suggested by Griffin and Ballagh[5] that the sounds caused by the
260 collision of raindrops depend on such parameters.

261 $L_{CRF}(RR)$ for site 1 was 10–15 dB higher than that for site 3. If the above
262 alternative reason was valid, then the leaves of the surrounding trees would
263 generate louder sounds by raindrop collision than gravel on the ground.

264 *Sites 2 and 4*

265 In the group of sites 2 and 4, both the absolute value and the slope were clearly
266 affected by the time period. For *NT*, $L_{CRF}(RR)$ increased by about 9–10 dB per
267 10-fold increase rainfall rate. The slopes for *DT* were shallower than those for
268 *NT*, and the slopes were 3–4 dB per 10-fold increase in rainfall rate.

269 As described in 3.2.3, traffic noise was dominant for *DT* at sites 2 and 4.
270 Ishikawa *et al.*[8] reported that the L_{Aeq} of noise from moving vehicles increased
271 by 2–5 dB under light rain conditions (average rainfall rate = 3 mm/h) compared
272 with that on sunny days, depending on the type of pavement (dense-graded or
273 drainage). The noise from moving vehicles on rainy days depends on puddles on
274 the road surface, and its relationship with the rainfall rate is not expected to be
275 explained by the same theory as that for the rain noise on roofs. Considering the
276 shallow slopes of $L_{CRF}(RR)$ for *DT*, the effect of the rainfall rate on the L_{Aeq} of
277 noise from moving vehicles should be small. Note that the pavements of the roads

278 adjacent to sites 2 and 4 were of the drainage type, suppressing the increase in
279 noise from moving vehicles due to rainfall[8].

280 For *NT*, the raindrop collision sound could have been more dominant than the
281 noise from moving vehicles because of the decrease in traffic volume, and as a
282 result, the slopes of $L_{CRF}(RR)$ might have approached those for the rain noise on
283 roofs. The difference in $L_{CRF}(RR)$ between *NT* and *DT* was around 15 dB for the
284 lowest rainfall rate, but it decreased with increasing rainfall rate. This indicates
285 that the raindrop collision sound in unusually heavy rain, such as a rainfall rate of
286 more than 100 mm/h, will exceed the noise from moving vehicles even for *DT*,
287 and the slopes for *DT* will become steeper under such conditions.

288 The higher $L_{CRF}(RR)$ for site 4 than for site 2 might be due to differences in
289 the surrounding buildings. There were large concrete buildings and many open
290 spaces around site 2, while there were wooden houses with a high density around
291 site 4 (see Fig. 1).

292 3.3.2. Relationship between rainfall rate and frequency characteristic of L_{eq}

293 To avoid redundancy by discussing all the statistical values, only the frequency
294 characteristic of the median of L_{eq} is analyzed as a representative characteristic
295 here. Figure 10 shows the median of L_{eq} for each 1/3 octave band and
296 classification shown in Table 3. Different symbols represent different rainfall rate
297 classifications. Dashed lines are the results for *without rainfall* shown in Fig. 7.

298 [Figure 10 about here.]

299 The median of L_{eq} increased with increasing rainfall rate mainly above
300 mid-frequencies of around 500 Hz to 1 kHz, though the frequency at which it
301 began to increase depended on the time period and site. From this result, it is

302 considered that the sounds caused by rainfall had stronger frequency components
 303 than the outdoor noise for *without rainfall* above the mid-frequencies, in the range
 304 of the rainfall rate observed in the present study. The effect of the rainfall rate on
 305 L_{eq} above mid-frequencies was smaller for *DT* than for *NT*, which was particularly
 306 clear for sites 2 and 4. This tendency was consistent with the slopes of $L_{CRF}(RR)$
 307 shown in Fig. 9.

308 To compare the frequency characteristics of the sounds caused by rainfall at
 309 the same rainfall rate, the band level of the sound for a certain rainfall rate was
 310 estimated. Firstly, $L_{CRF}(RR, i)$, which is the band level of the sounds caused by
 311 rainfall with a rainfall rate of RR for band i , was calculated as

$$L_{CRF}(RR, i) = 10 \log_{10} \left(10^{L_{eq}(RR, i)/10} - 10^{L_{eq}(0, i)/10} \right), \quad (2)$$

312 where $L_{eq}(0, i)$ is the median of L_{eq} without rainfall for band i and $L_{eq}(RR, i)$
 313 is the median of L_{eq} for band i where the median of the rainfall rate is RR .
 314 Then, $\hat{L}_{CRF}(RR, i)$ for a certain RR was estimated by linear regression analysis
 315 between $L_{CRF}(RR, i)$ and the median rainfall rate for each band. The estimated
 316 level was adopted when the correlation coefficient for the regression analysis was
 317 statistically different from zero ($p = 0.05$), in other words, when the correlation
 318 coefficient was larger than 0.997, 0.950, and 0.878 for 3, 4, and 5 samples,
 319 respectively.

320 Figure 11 shows $\hat{L}_{CRF}(RR, i)$ for RR values of 3 and 30 mm/h. These two RR
 321 values were respectively chosen to represent light and heavy rain conditions within
 322 the range of interpolation or slight extrapolation of the regression equations.
 323 Considering the results of $L_{CRF}(RR)$ shown in Fig. 9, the results of $\hat{L}_{CRF}(RR, i)$
 324 are divided into the two groups of sites and analyzed.

[Figure 11 about here.]

Sites 1 and 3

For both sites 1 and 3, $\hat{L}_{\text{CRF}}(RR, i)$ in *DT* was slightly higher than that in *NT* for *RR* of 3 mm/h, but the differences almost disappeared for *RR* of 30 mm/h. This tendency was expected from the regression lines shown in Fig. 9. The frequency characteristics for *RR* of 30 mm/h can be regarded as those for the sound caused by raindrop collisions because $\hat{L}_{\text{CRF}}(RR, i)$ in *DT* was almost the same as that in *DT*. The characteristics were similar for sites 1 and 3. The characteristics were almost flat within the range of 1–4 kHz and decayed at higher frequencies. However, the absolute values for site 1 were 5–10 dB higher than those for site 3, and it is highly probable that this was caused by the difference in the type of object against which raindrops collided, as mentioned in 3.3.1.

Sites 2 and 4

In many cases, $\hat{L}_{\text{CRF}}(RR, i)$ could not be obtained at medium or low frequencies because the median of L_{eq} did not depend on the rainfall rate at these frequencies. For *RR* of 3 mm/h, at frequencies above 1 kHz, the frequency characteristics showed steep slopes and $\hat{L}_{\text{CRF}}(RR, i)$ decreased about 6 to 8 dB with a doubling of the center frequency of 1/3 octave band. $\hat{L}_{\text{CRF}}(RR, i)$ in *DT* was clearly higher than that in *NT*, though the difference was smaller for site 4 owing to the shallow slope in *NT* relative that for site 2. For *RR* of 30 mm/h, there were differences between sites 2 and 4. For site 2, the characteristics retained their steep slopes and the clear difference in $\hat{L}_{\text{CRF}}(RR, i)$ for different time periods. For site 4, the slopes became shallower than those for *RR* of 3 mm/h in both time periods, and $\hat{L}_{\text{CRF}}(RR, i)$ in *NT* approached that in *DT*. The negligible difference in $\hat{L}_{\text{CRF}}(RR, i)$ between *NT* and

349 *DT* with different traffic volumes suggests that the raindrop collision sound was
350 more dominant than the traffic noise.

351 From the above results, it can be concluded that the steep slope was due to
352 noise from moving vehicles on a wet road, whereas the shallow slope observed at
353 site 4 was the result of an increase in the energy of the raindrop collision sound
354 relative to that of traffic noise. This is consistent with the inference in 3.3.1 that the
355 effect of the raindrop collision sound was stronger at site 4 than at site 2 because
356 of the high density of surrounding buildings.

357 4. General discussion

358 4.1. Macroscopic model of outdoor noise under rainy condition

359 The measurement results demonstrated that the rainfall rate affected the traffic
360 noise and raindrop collision sound differently, and that the SPL of the raindrop
361 collision sound depended on the surface material in the surrounding environment.
362 In addition, the effect of the rainfall rate became strong as the SPL for *without*
363 *rainfall* decreased. From these results, it is worth considering the following
364 macroscopic model to estimate the SPL of outdoor noise under rainy conditions:

$$L(RR) = 10 \log_{10} \sum_{k=1}^n E_k RR^{a_k}, \quad (3)$$

365 where $L(RR)$ is the SPL of outdoor noise when the rainfall rate is RR , E_k is the
366 sound energy for element k , which constitutes outdoor noise at a rainfall rate of
367 1 mm/h, and a_k is a parameter that determines the effect of the rainfall rate on
368 element k .

369 a_k is a real number greater than or equal to zero (assuming that $0^0 = 1$). As
370 a_k approaches zero, the sound energy of the element approaches a constant value

371 regardless of the rainfall rate, and as a_k becomes larger, the sound energy of the
372 element more rapidly increases with increasing rainfall rate. When outdoor noise
373 consists of a single element ($n = 1$), the SPL of the outdoor noise increases by
374 $10a_1$ dB per 10-fold increase in rainfall rate.

375 If element k represents traffic noise, E_k will be determined by the traffic
376 volume and the type of pavement, while a_k will only be determined by the type
377 of pavement. If element k represents the raindrop collision sound, E_k will be
378 determined by the physical properties of the collision surface, while a_k will be
379 determined by the number of collisions per unit time and the size of raindrops.

380 We attempted to estimate the median of L_{Aeq} from this model. The elements
381 constituting outdoor noise were classified into sound existing regardless of the
382 presence or absence of rainfall and sound resulting from rainfall, and the latter
383 was further divided into two sounds derived from the change in the road surface
384 condition (dry/wet/with puddles) and raindrop collisions.

385 The sound existing regardless of the presence or absence of rainfall was
386 estimated from the results of *without rainfall* shown in Fig. 8 (horizontal solid
387 line). a_k is zero for this sound.

388 The sound derived from raindrop collisions was estimated from the results of
389 Fig. 9 in NT as the closest value. E_k was the constant term of the regression
390 equation in Fig. 9, that is, the estimated value of $L_{CRF,1mm/h}$. a_k was obtained by
391 dividing the slope of the regression equation by 10.

392 For the sound derived from the change in the road surface condition,
393 estimations of E_k and a_k were difficult. Here, E_k in NT was set to zero, and
394 that in DT was obtained from the energy difference between the constant terms
395 of the regression equations for DT and NT . The values of a_k for sites 2 and 4

were obtained by dividing the slope of the regression equation for DT , that is, the measurement time during which traffic noise was dominant, by 10. The values of a_k for sites 1 and 3 were set at 0.3, which is the average of the values for sites 2 and 4, because the effect of traffic noise was unknown. For example, Eq. 4 describes the model of $L(RR)$ for site 1 in DT .

$$L(RR) = 10 \log_{10} \left(10^{51.5/10} RR^0 + 10^{45.4/10} RR^{0.834} + (10^{50.1/10} - 10^{45.4/10}) RR^{0.3} \right) \quad (4)$$

Figure 12 shows the medians of L_{Aeq} estimated from the macroscopic model for each pair of site and time period. The measured values were equal to those shown in Fig. 8. The determination coefficients between the measured and estimated values ranged from 0.83 to 0.99, and the overall shapes of the measured values and estimated curves coincided for all pairs of site and time period. Therefore, it can be concluded that the macroscopic model was valid within the range of the data obtained in the present study, though there is still much room to optimize the sound classification and estimation methods for each parameter.

[Figure 12 about here.]

4.2. Effect of rainfall on outdoor acoustic mass notification system

In this section, the maximum distances from the loudspeaker to maintain a certain speech-to-noise ratio in heavy rain are estimated to discuss the effect of rainfall on an outdoor acoustic mass notification system. The speech-to-noise ratio here is defined as the difference in L_{Aeq} between the amplified speech provided by the system and the background noise at the listening point.

417 Table 5 shows the medians of L_{Aeq} estimated from the macroscopic model
 418 shown in Fig. 12 for rainfall rates of 0, 40, 80, and 160 mm/h. These values were
 419 used as the background noise level regardless of the distance from the loudspeaker
 420 to calculate the speech-to-noise ratio.

421 [Table 5 about here.]

422 Next, we estimate the speech level at a certain distance from the speaker of the
 423 system. First, we quantify the effect of atmospheric absorption on the A-weighted
 424 SPL of speech. Atmospheric absorption coefficients in ISO 9613-1:1993[15] for
 425 a temperature of 15°C and a relative humidity of 90% were used, considering
 426 the measured data shown in Table 4. Although the relative humidity dropped to
 427 about 60 to 70% for *without rainfall*, the combination of the above temperature
 428 and relative humidity was used for all conditions because there was almost no
 429 difference observed in the results. The frequency characteristic of speech was
 430 assumed to be that for the vocal effort of *Normal* given in the standard for
 431 calculating the speech intelligibility index (SII)[16]. In the calculation example
 432 here, the data in 1/3 octave bands from 160 Hz to 8 kHz were used. When a
 433 point 1 m from the loudspeaker is the reference point, the attenuation of the
 434 A-weighted SPL of speech due to the atmospheric absorption at a point of r m
 435 from the loudspeaker ($\Delta L_{A,absb}(r)$) can be obtained as

$$\Delta L_{A,absb}(r) = 10 \log_{10} \sum_{i=1}^{18} 10^{\frac{L_{i,Normal}(1) - \alpha_i(r-1) + Aw_i}{10}} - L_{A,Normal}(1), \quad (5)$$

436 where α_i dB/m is the atmospheric absorption coefficient for band i , Aw_i dB is the
 437 A-weighting correction value for band i , $L_{i,Normal}(1)$ is the SPL of speech with
 438 *Normal* vocal effort for band i at a distance of 1 m from the loudspeaker, and

439 $L_{A,Normal}(1)$ dB is the A-weighted SPL of speech at a distance of 1 m from the
 440 loudspeaker. $L_{A,Normal}(1)$ can be obtained from the energy sum of $L_{i,Normal}(1) +$
 441 Aw_i . Using the values given in the standard for SII, $L_{A,Normal}(1)$ is calculated to
 442 be 59.2 dB. Figure 13 shows $\Delta L_{A,absb}(r)$ at distances from 1 to 5000 m obtained
 443 using Eq. 5.

444 [Figure 13 about here.]

445 The A-weighted SPL of amplified speech at a distance of r m from the
 446 loudspeaker ($L_A(r)$) can be obtained from Eq. 6, assuming that the loudspeaker
 447 is omnidirectional and that the distance attenuation does not depend on the sound
 448 frequency.

$$L_A(r) = L_A(1) + \Delta L_{A,absb}(r) - 20 \log_{10} r \quad (6)$$

449 Here, $L_A(1)$ [dB/m] is the A-weighted SPL of amplified speech. For the
 450 loudspeakers used in Japan, the maximum SPL at a distance of 1 m from the
 451 loudspeaker is around 125 dB. When the SPL of amplified speech with the
 452 frequency characteristic of *Normal* vocal effort is 125 dB, its A-weighted SPL
 453 is calculated to be 121.9 dB. Therefore, $L_{A, 1m}$ is set to 121.9 dB.

454 Table 6 shows the maximum distances from the loudspeaker to maintain a
 455 speech-to-noise ratio of more than +6 dB, as examples criteria to ensure a certain
 456 degree of intelligibility. For each combination of site, time period, and rainfall
 457 rate, values were determined in 1 m steps, using the ratio obtained by subtracting
 458 the estimated background noise level shown in Table 5 from $L_A(r)$. Under no
 459 rainfall condition, the ratio of +6 dB or more can be achieved, even at a distance
 460 on the order of kilometers, except for sites 2 and 4 in *DT* where traffic noise was

461 dominant. However, under heavy rain conditions such as a rainfall rate of more
462 than 40 mm/h, the maximum distances decreased to the order on 100 m regardless
463 of the site and time period.

464 These calculations clearly show that it is necessary to devise a means of coping
465 with such a reduction in the coverage of the loudspeaker due to heavy rain. For
466 example, the design of a system with a margin for the maximum sound output
467 by spatially densifying the loudspeaker arrangement or adopting a loudspeaker
468 with less distance attenuation may be possible. Moreover, the introduction of a
469 movable mass notification system, such as a car, an unmanned aerial vehicle, is
470 also worth considering.

471 [Table 6 about here.]

472 5. Conclusion

473 In the present study, long-term surveys of rainfall rate and outdoor noise
474 were conducted at four sites with different surrounding environments and the
475 relationship between them was analyzed to clarify the effects of the rainfall rate
476 on the physical characteristics of outdoor noise. The results are summarized as
477 follows.

478 (1) L_{Aeq} tended to increase linearly with the logarithm of the rainfall rate;
479 however, the slopes were different at different sites and time periods. The
480 slopes became steep as L_{Aeq} for the no rain condition decreased because the
481 raindrop collision sound became more dominant than other sounds.

482 (2) The L_{eq} for each 1/3 octave band increased with increasing rainfall rate,
483 mainly above mid-frequencies of around 500 Hz to 1 kHz, though the

484 frequencies at which the level began to increase depended on the site and
485 time period.

486 (3) A macroscopic model for estimating the sound pressure level under rainy
487 conditions was proposed, and its validity was confirmed from the high
488 determination coefficients of 0.83 to 0.99 within the range of the data
489 obtained in the present study.

490 (4) Calculations of the coverage of outdoor acoustic mass notification systems
491 indicated that the distance to ensure a certain speech-to-noise ratio could be
492 significantly reduced by heavy rainfall.

493 **Acknowledgments**

494 The research was partially funded by the Promotion Program for Scientific
495 Fire and Disaster Prevention Technologies of the Fire and Disaster Management
496 Agency of Japan (2015). The authors would like to thank Itami City and Itami
497 City Fire Department for their cooperation in the long-term field measurement.

[1] L. N. Miller, Sound levels of rain and of wind in the trees, *Noise Control Eng. J.* 11 (1978) 101–115.

[2] P. Dubout, The sound of rain on a steel roof, *Journal of Sound and Vibration* 10 (1) (1969) 144–150.

[3] K. Ballagh, Noise of simulated rainfall on roofs, *Applied Acoustics* 31 (1990) 245–264.

- [4] J. McLoughlin, D. J. Saunders, R. D. Ford, Noise generated by simulated rainfall on profiled steel roof structures, *Applied Acoustics* 42 (1994) 239–255.
- [5] D. Griffin, K. Ballagh, A consolidated theory for predicting rain noise, *Journal of Building Acoustics* 19 (4) (2012) 221–248.
- [6] Y. Xiang, L. Shuai, L. Junjie, Experimental studies on the rain noise of lightweight roofs: Natural rains vs artificial rains, *Applied Acoustics* 106 (2016) 63–76.
- [7] E. F. Freitas, P. A. A. Pereira, L. G. P. Santos, A. P. S. Santos, Traffic noise changes due to water on porous and dense asphalt surfaces, *Road Materials and Pavement Design* 10 (3) (2009) 587–607.
- [8] K. Ishikawa, R. Fukui, H. Nagaoka, E. Noguchi, J. Inoue, A study on the acoustical property of drainage porous asphalt pavement in rain, *Proc. of the Meeting the Institute of Noise Control Engineering of Japan* (2010) 140–142 (in Japanese).
- [9] J. Alonso, J. M. López, I. Pavón, M. Recuero, C. Asensio, G. Arcas, A. Bravo, On-board wet road surface identification using tyre/road noise and Support Vector Machines, *Applied Acoustics* 76 (2014) 407–415.
- [10] M. Cai, S. Zhong, H. Wang, Y. Chen, W. Zeng, Study of the traffic noise source intensity emission model and the frequency characteristics for a wet asphalt road, *Applied Acoustics* 123 (2017) 55–63.
- [11] ISO 10140-5:2010 Am1:2014 Acoustics – Laboratory measurement of

sound insulation of building elements – Part 5: Requirements for test facilities and equipment AMENDMENT 1: Rainfall sound, 2014.

- [12] G. F. Hessler, D. M. Hessler, P. Brandstätter, K. Bay, Experimental study to determine wind-induced noise and windscreen attenuation effects on microphone response for environmental wind turbine and other applications, *Noise Control Eng. J.* 56 (4) (2008) 300–309.
- [13] I.-C. Lin, Y.-R. Hsieh, P.-F. Shieh, H.-C. Chuang, H.-C., L.-C. Chou, The effect of wind on low frequency noise, *Proc. of Inter Noise 2014* (2014) 1–12.
- [14] The Research Committee on Road Traffic Noise in the Acoustical Society of Japan, ASJ Prediction Model 2008 for road traffic noise: Report from the Research Committee on Road Traffic Noise in the Acoustical Society of Japan, *J. Acoust. Jpn.* 65 (4) (2009) 179–232 (in Japanese).
- [15] ISO 9613-1:1993 Acoustics – Attenuation of sound during propagation outdoors – Part 1: Calculation of the absorption of sound by the atmosphere, 1993.
- [16] ANSI S3.5-1997, American National Standard Methods for the Calculation of the Speech Intelligibility Index, 1997.

List of Figures

1	Satellite photos of the measurement sites obtained from Google Earth. The measurements were performed at the red circle in each photo.	28
2	Example of installed equipment (Site 2).	29
3	Temporal sequence of rainfall rate for each site. Periods colored in grey represent missing observations.	30
4	Time sequences of L_{Aeq} for the week from 2nd to 8th Nov. 2015. Samples of <i>with rainfall</i> were omitted.	31
5	Time sequence of statistics of L_{Aeq} without rainfall for each site. Solid and dashed lines represent the median and 90% range, respectively.	32
6	Effect of wind speed on L_{Aeq} without rainfall for each site and time period. The upper panel shows the median of L_{Aeq} as a function of wind speed, and the lower panel shows the cumulative frequency of wind speed.	33
7	1/3 Octave band spectrum of statistics of L_{eq} without rainfall for each site and time period. Solid and dashed lines represent the median and 90% range, respectively.	34
8	Relationship between rainfall rate and L_{Aeq} . Solid and dashed lines represent the median and 90% range of L_{Aeq} for <i>without rainfall</i> respectively. Circles and error bars represent the median and 90% range of L_{Aeq} and rainfall rate for <i>with rainfall</i> , respectively.	35
9	Relationship between rainfall rate and L_{Aeq} of the sounds caused by rainfall ($L_{CRF}(RR)$). Solid and dashed lines represent regression lines for each condition. Different symbols represent different pairs of site and time period.	36
10	1/3 Octave band spectrum of the median of L_{eq} with rainfall for each site and time period. Dashed lines represent L_{eq} for <i>without rainfall</i> as a reference. Different symbols represent different rainfall rate (RR) classifications.	37
11	Estimated L_{eq} of the sounds caused by rainfall for each 1/3 octave band. Left and right panels show results for rainfall rates (RR s) of 3 and 30 mm/h, respectively. Different symbols represent different pairs of site and time period.	38

12	Measured and estimated medians of L_{Aeq} for each pair of site and time period. The estimated values were obtained from the macroscopic model defined by Eq. 3.	39
13	Attenuation of A-weighted level of speech by atmospheric absorption as a function of distance from loudspeaker ($\Delta L_{A,absb}$), where temperature is 15°C and relative humidity is 90%.	40



Figure 1: Satellite photos of the measurement sites obtained from Google Earth. The measurements were performed at the red circle in each photo.

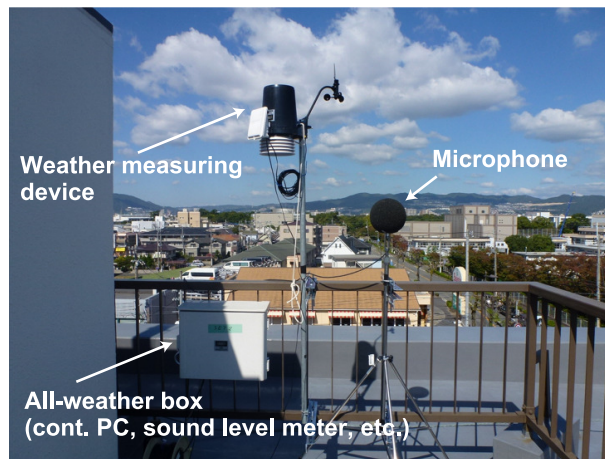


Figure 2: Example of installed equipment (Site 2).

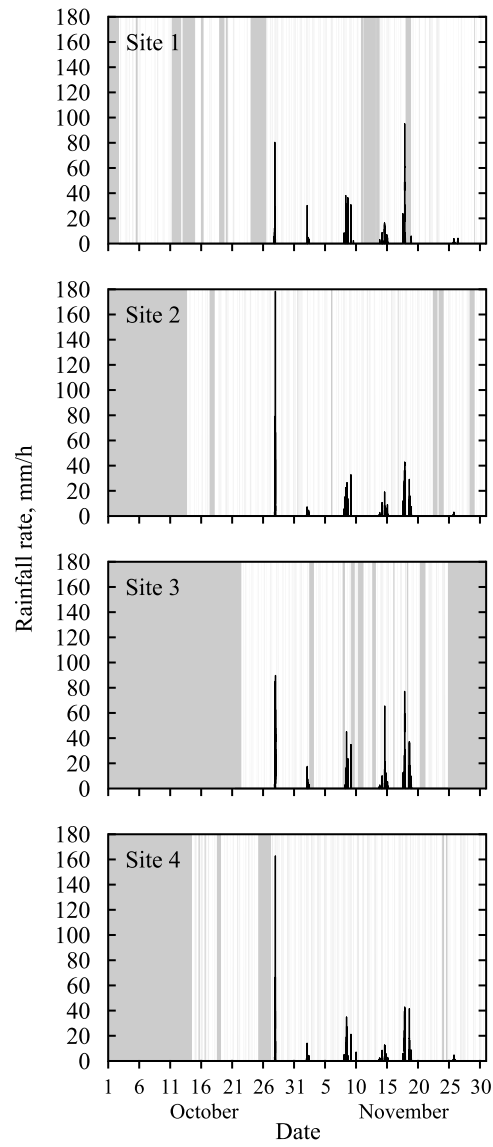


Figure 3: Temporal sequence of rainfall rate for each site. Periods colored in grey represent missing observations.

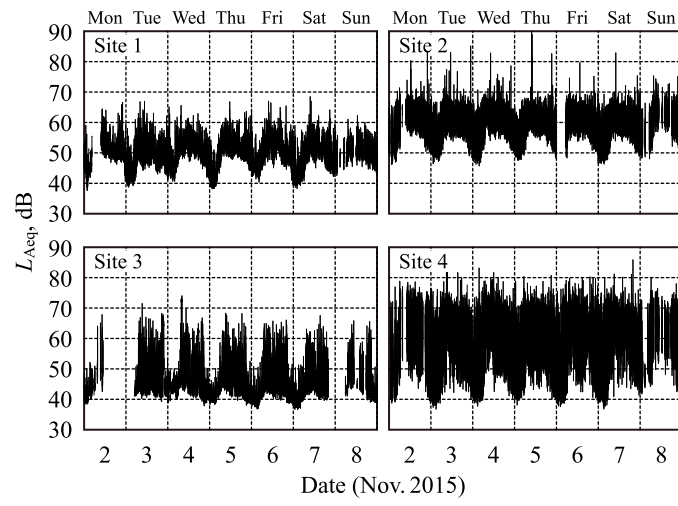


Figure 4: Time sequences of L_{Aeq} for the week from 2nd to 8th Nov. 2015. Samples of *with rainfall* were omitted.

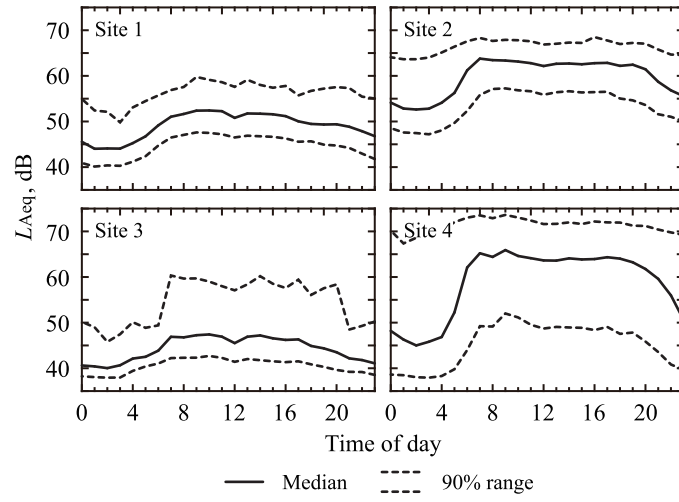


Figure 5: Time sequence of statistics of L_{Aeq} without rainfall for each site. Solid and dashed lines represent the median and 90% range, respectively.

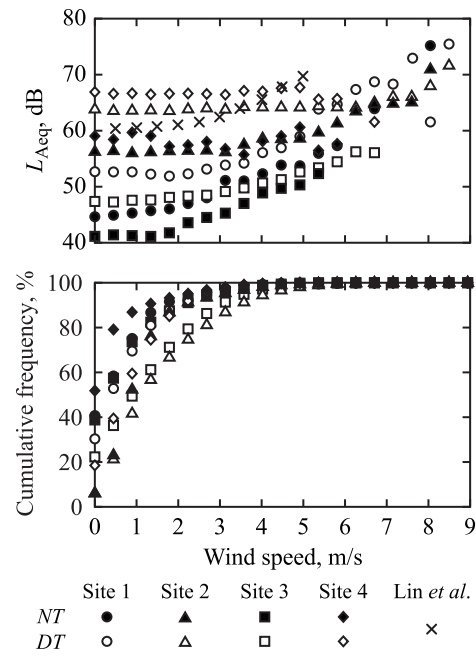


Figure 6: Effect of wind speed on L_{Aeq} without rainfall for each site and time period. The upper panel shows the median of L_{Aeq} as a function of wind speed, and the lower panel shows the cumulative frequency of wind speed.

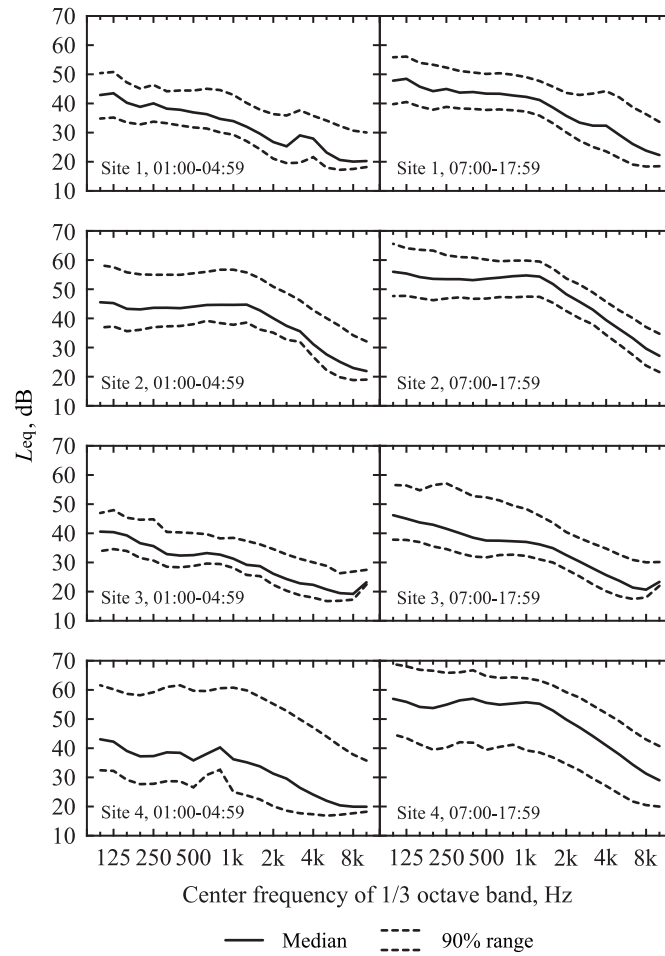


Figure 7: 1/3 Octave band spectrum of statistics of L_{eq} without rainfall for each site and time period. Solid and dashed lines represent the median and 90% range, respectively.

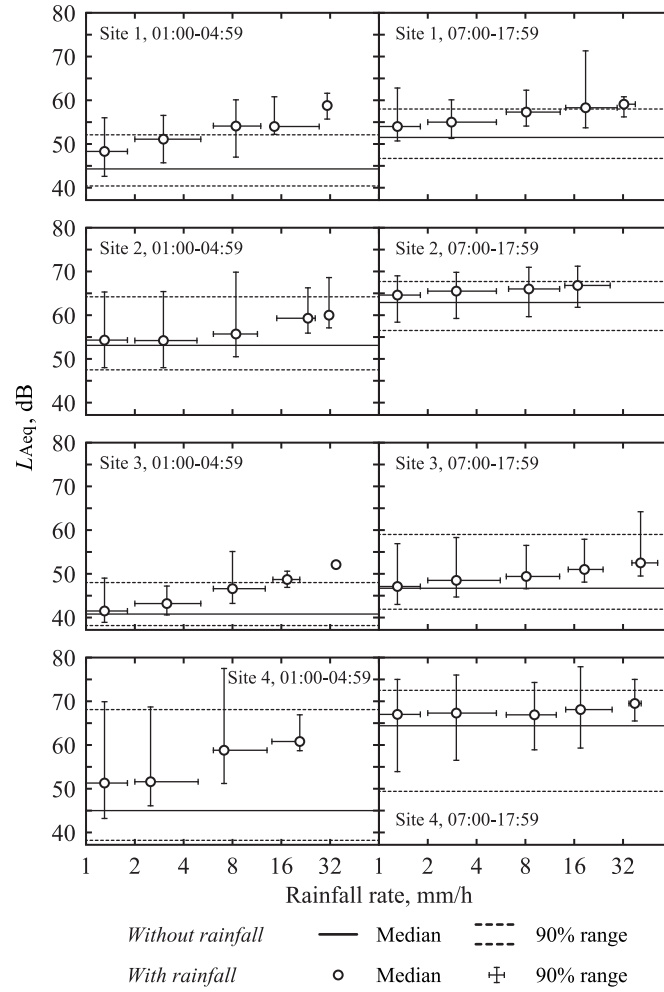


Figure 8: Relationship between rainfall rate and L_{Aeq} . Solid and dashed lines represent the median and 90% range of L_{Aeq} for *without rainfall* respectively. Circles and error bars represent the median and 90% range of L_{Aeq} and rainfall rate for *with rainfall*, respectively.

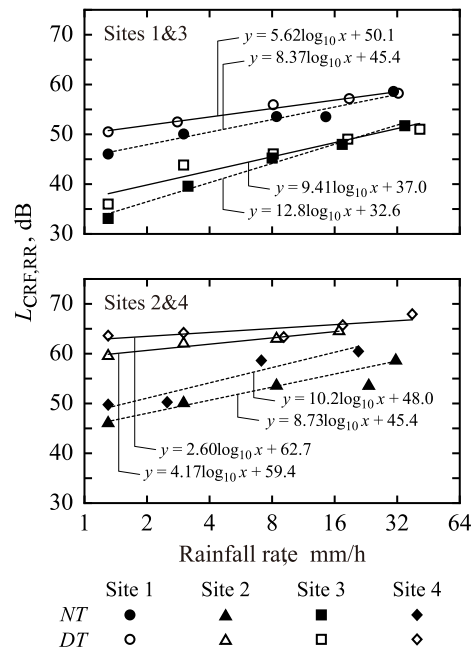


Figure 9: Relationship between rainfall rate and L_{Aeq} of the sounds caused by rainfall ($L_{CRF}(RR)$). Solid and dashed lines represent regression lines for each condition. Different symbols represent different pairs of site and time period.

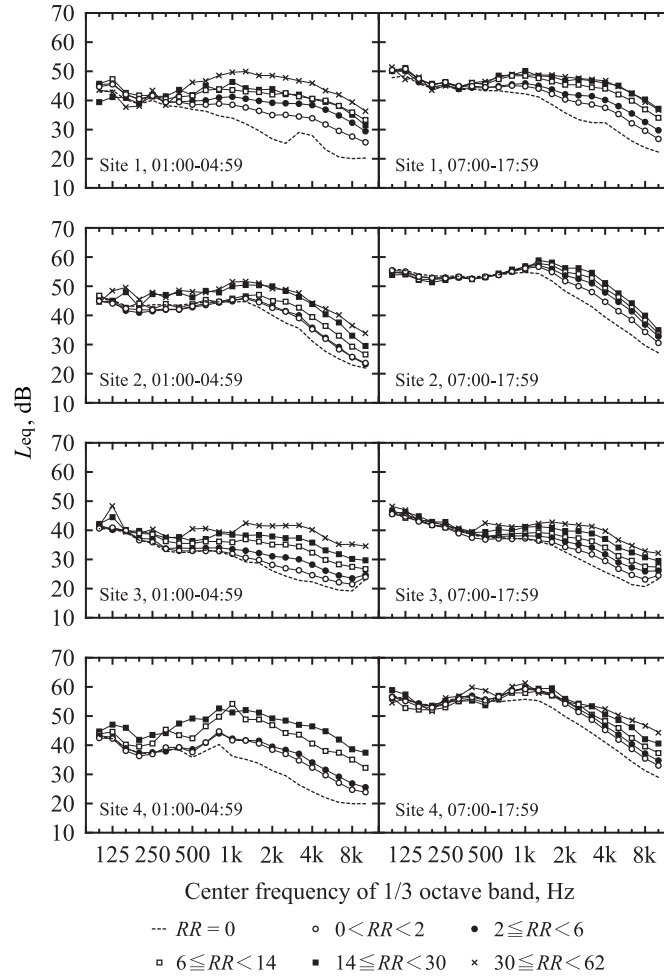


Figure 10: 1/3 Octave band spectrum of the median of L_{eq} with rainfall for each site and time period. Dashed lines represent L_{eq} for *without rainfall* as a reference. Different symbols represent different rainfall rate (RR) classifications.

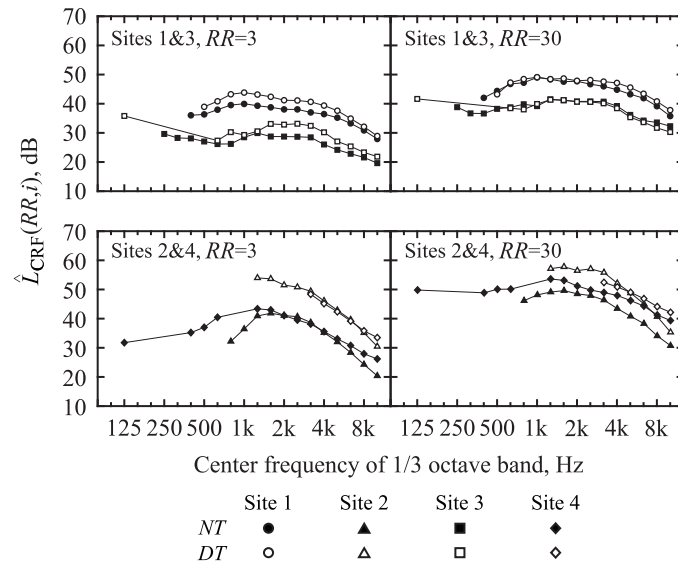


Figure 11: Estimated L_{eq} of the sounds caused by rainfall for each 1/3 octave band. Left and right panels show results for rainfall rates (RR s) of 3 and 30 mm/h, respectively. Different symbols represent different pairs of site and time period.

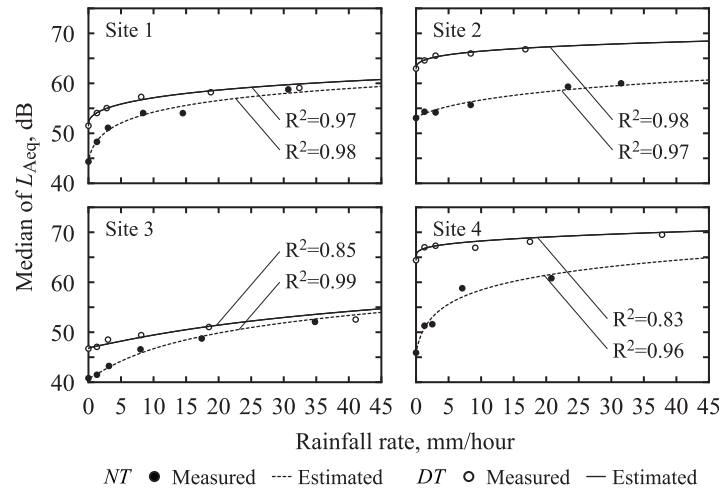


Figure 12: Measured and estimated medians of L_{Aeq} for each pair of site and time period. The estimated values were obtained from the macroscopic model defined by Eq. 3.

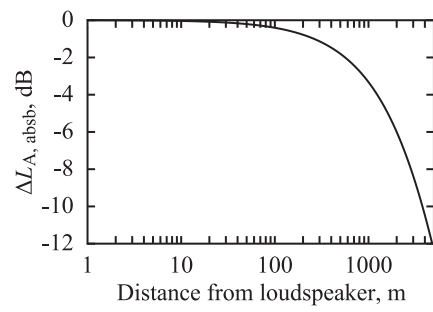


Figure 13: Attenuation of A-weighted level of speech by atmospheric absorption as a function of distance from loudspeaker ($\Delta L_{A, \text{absb}}$), where temperature is 15°C and relative humidity is 90%.

List of Tables

1	Summary of the measurement sites.	42
2	Number of samples and measurement periods for each site. Data were sampled every minute. The columns of ‘> 0 mm/h’ and ‘> 40 mm/h’ indicate the number of samples with rainfall and that with heavy rainfall, respectively.	43
3	Classification of rainfall rate in the present study and number of samples for each site and time period. <i>NT</i> and <i>DT</i> are time periods of 01:00–04:59 and 07:00–17:59, respectively.	44
4	Representative values of weather parameters for each classification of rainfall rate. The classification of zero means <i>without rainfall</i> . The values for rainfall rate, temperature, and relative humidity are medians, and that for wind speed is average.	45
5	L_{Aeq} estimated from the macroscopic model under the no rain and heavy rain conditions.	46
6	Maximum distance from loudspeaker to maintain the speech-to-noise ratio of +6 dB under the no rain and heavy rain conditions.	47

Table 1: Summary of the measurement sites.

Site	Installation location	Surroundings
1	Rooftop (2 levels)	On campus, many trees, quiet with few pedestrians
2	Rooftop (3 levels)	Beside major road with microphone installed some distance from road
3	1.5 m above ground	Vacant lot covered with gravel, periodic aircraft noise
4	Sidewall on 2nd floor	Beside major road with microphone installed close to road

Table 2: Number of samples and measurement periods for each site. Data were sampled every minute. The columns of ‘> 0 mm/h’ and ‘> 40 mm/h’ indicate the number of samples with rainfall and that with heavy rainfall, respectively.

Site	Measurement period	Number of samples		
		Total	> 0 mm/h	> 40 mm/h
1	Oct. 2, 2015–Nov. 30, 2015	66,808	2,358	13
2	Oct. 13, 2015–Nov. 30, 2015	63,068	2,681	17
3	Oct. 21, 2015–Nov. 24, 2015	41,001	2,418	25
4	Oct. 14, 2015–Nov. 30, 2015	61,627	2,551	10

Table 3: Classification of rainfall rate in the present study and number of samples for each site and time period. *NT* and *DT* are time periods of 01:00–04:59 and 07:00–17:59, respectively.

Classification	Rainfall rate (<i>RR</i>), mm/h	Site 1		Site 2		Site 3		Site 4	
		<i>NT</i>	<i>DT</i>	<i>NT</i>	<i>DT</i>	<i>NT</i>	<i>DT</i>	<i>NT</i>	<i>DT</i>
1	$0 < RR < 2$	222	400	205	521	71	422	166	599
2	$2 \leq RR < 6$	211	369	148	494	42	553	144	486
3	$6 \leq RR < 14$	20	79	23	108	16	167	10	79
4	$14 \leq RR < 30$	5	15	4	28	8	31	5	17
5	$30 \leq RR < 62$	3	6	4	0	1	6	0	3

Table 4: Representative values of weather parameters for each classification of rainfall rate. The classification of zero means *without rainfall*. The values for rainfall rate, temperature, and relative humidity are medians, and that for wind speed is average.

Parameter	Classification	Site 1		Site 2		Site 3		Site 4	
		<i>NT</i>	<i>DT</i>	<i>NT</i>	<i>DT</i>	<i>NT</i>	<i>DT</i>	<i>NT</i>	<i>DT</i>
Rainfall rate, mm/h	0	0.0	0.0	0.0	0.0	0.0	0.0	0.0	0.0
	1	1.3	1.3	1.3	1.3	1.3	1.3	1.3	1.3
	2	3.0	2.8	3.0	3.0	3.0	3.0	2.5	3.0
	3	8.4	8.1	8.4	8.4	8.0	8.1	7.1	9.1
	4	14.5	18.8	23.4	16.8	17.4	18.7	20.8	17.5
	5	30.7	32.4	31.5	-	34.8	41.1	-	37.8
Temperature, °C	0	15.9	18.5	13.4	17.8	14.3	17.8	13.2	17.7
	1	17.2	17.4	17.2	17.1	16.4	16.9	16.9	16.8
	2	17.2	17.6	17.4	17.1	16.9	17.1	16.9	16.8
	3	17.2	18.2	17.2	17.2	12.4	17.1	17.6	16.8
	4	18.6	18.2	17.8	16.9	17.9	17.1	17.6	16.7
	5	19.2	18.0	17.8	-	17.9	17.2	-	16.7
Relative humidity, %	0	77.0	67.0	83.0	66.0	81.0	65.0	83.0	66.0
	1	89.0	92.5	93.0	94.0	95.0	92.0	93.0	94.0
	2	88.0	93.0	91.0	95.0	95.0	92.0	90.0	94.0
	3	88.0	93.0	96.0	95.0	89.0	92.0	97.0	94.0
	4	95.0	93.0	97.0	94.5	95.0	92.0	97.0	94.0
	5	94.0	93.5	97.0	-	95.0	92.0	-	94.0
Wind speed, m/s	0	0.7	0.9	1.3	1.7	0.8	1.4	0.5	1.1
	1	1.1	0.9	0.9	1.2	0.6	0.5	0.6	0.7
	2	1.1	0.8	0.8	1.2	0.7	0.5	0.5	0.7
	3	1.7	0.8	0.7	1.8	1.1	0.8	0.0	1.5
	4	0.5	1.0	0.5	2.3	0.6	0.8	0.0	1.2
	5	0.4	0.8	0.3	-	0.0	1.7	-	1.3

Table 5: L_{Aeq} estimated from the macroscopic model under the no rain and heavy rain conditions.

Rainfall rate, mm/h	Site 1		Site 2		Site 3		Site 4	
	<i>NT</i>	<i>DT</i>	<i>NT</i>	<i>DT</i>	<i>NT</i>	<i>DT</i>	<i>NT</i>	<i>DT</i>
0	44.3	51.5	53.1	62.9	40.8	46.7	45.9	64.4
40	59.0	60.4	60.3	68.3	53.4	54.2	64.4	70.1
80	61.4	62.4	62.5	69.4	57.1	57.4	67.4	71.4
160	63.9	64.6	64.9	70.7	60.9	61.0	70.5	73.2
[dB]								

Table 6: Maximum distance from loudspeaker to maintain the speech-to-noise ratio of +6 dB under the no rain and heavy rain conditions.

Rainfall rate, mm/h	Site 1		Site 2		Site 3		Site 4	
	<i>NT</i>	<i>DT</i>	<i>NT</i>	<i>DT</i>	<i>NT</i>	<i>DT</i>	<i>NT</i>	<i>DT</i>
0	1,385	854	759	335	1,704	1,189	1,252	292
40	473	419	423	201	742	698	292	168
80	384	351	348	180	554	541	219	147
160	306	286	279	158	401	398	161	122

[m]